A Simple Structure Orthomode Transducer for Millimeter-Wave Applications

Tanner J. Douglas, Adib Y. Nashashibi, Hussein N. Shaman, and Kamal Sarabandi

Abstract – This article presents the design of an orthomode transducer (OMT) with a simple structure for ease of fabrication at the 230 GHz band. The structure consists of a square waveguide T junction with transitions to rectangular waveguides for the V- and H-polarized ports. The design is facilitated by a numerical simulation tool based on the finite element method. This OMT features the simplest possible configuration amenable for standard computer numerical control machining for operation at the *J* band (consistent with WR-03 waveguide standard). The fabricated and measured OMT exhibits an operational bandwidth of 12%, over which greater than 10 dB return loss and greater than 30 dB cross-polarization isolation are achieved. The insertion loss is minimized to an average less than 2 dB using time-extended electroless gold plating to improve the surface conductivity and fill the waveguides' seams. This OMT is integrated within a fully polarimetric radar operating at 220 GHz to 230 GHz.

1. Introduction

Millimeter-wave radars are one of the many sensor systems used in the automotive industry for driver assistance and autonomous vehicle operation. Radar offers benefits over optical imaging and lidar, including longer range and penetration through inclement weather conditions. In addition, radar can exploit polarimetry to discriminate between targets based on their polarization response [1, 2]. Although current automotive radars operate at the 77 GHz band, there is interest in using the 230 GHz band for future systems [3]. With the advent of semiconductor and microfabrication technologies, realization of such high-frequency radars is becoming viable [4, 5]. Polarimetric radars often make use of antennas that support dual polarization for either transmit or receive or both. In such systems, an orthomode transducer (OMT) is required to manage electromagnetic signals in vertical and horizontal polarizations.

All OMTs need to combine two orthogonal waveguides into a common waveguide that can support a degenerate mode. According to the literature, many groups have accomplished this, with varying levels of fabrication difficulty and performance characteristics. The aim of this article is to design the simplest structure with the minimum number of fabrication steps and waveguide seams, with the goal of achieving a high-performance and low-cost OMT that can be manufactured by a standard computer numerical control (CNC) milling machine.

It is challenging to design and fabricate OMTs with the desired level of performance at millimeter-wave frequencies due to the tiny dimensions of the waveguides. Several different designs for OMTs at these frequency ranges were reported and achieved outstanding performance over a wide bandwidth. Some such designs use a T-junction structure [6, 7] but involve many different machined steps requiring very high precision. Other designs implement a reverse-coupling structure [8, 9], a finline guide [10], a Bøifot junction [11–13], or a three-dimensional turnstile junction [14–18]. These techniques require specialty machining equipment or complex multilayer silicon micromachining processes to fabricate, can be costly, and have poor yield.

This article presents an OMT design for operation at 220 GHz to 230 GHz. The geometric simplicity of this OMT allows it to be constructed by CNC machining with modest equipment and can be manufactured with better performance, at higher frequencies, and for lower cost than can be found in the commercial millimeter-wave component market. It also avoids the aforementioned complex structures, reducing the necessary number of high-precision machined waveguide sections. A fabricated prototype was produced with excellent electromagnetic characteristics over a bandwidth of 12%. Preliminary results of this design can be found in [19]. Subsequently, we have improved the fabrication process resulting in much improved insertion loss, expanded the bandwidth significantly, and adjusted the measurement setup to allow a more complete characterization of device performance.

The T-junction structure used for this OMT is one that was previously examined [6, 7], and drawbacks of the split-block assembly fabrication technique were identified [6, 17]. In addition, this design compromises performance, particularly in terms of bandwidth, compared with the designs listed previously. However, for engineers and researchers without access to top-of-the-line machining equipment required to fabricate the small features of these high-performing but complex OMT designs at millimeter-wave frequencies, our design presents an alternative that can be easily fabricated with performance suitable for narrower band

Manuscript received 22 December 2022.

Tanner J. Douglas, Adib Y. Nashashibi, and Kamal Sarabandi are with the Electrical Engineering and Computer Science Department, University of Michigan, 1301 Beal Ave, Ann Arbor, Michigan 48109, USA; e-mail: tjdoug@umich.edu, nuha@umich.edu, saraband@umich.edu.

Hussein N. Shaman is with the Center of Excellence for Microwave Sensor Technology, King Abdulaziz City for Science and Technology, King Abdullah Rd, Al Raed, Riyadh 12371, Saudi Arabia; e-mail: hshaman@kacst.edu.sa.

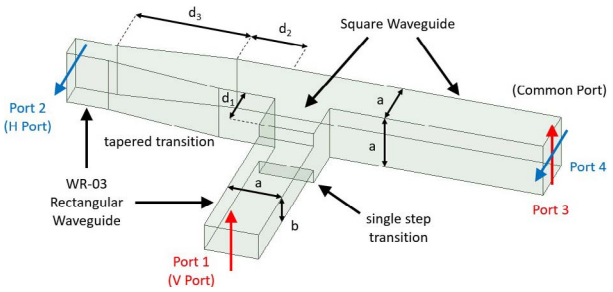

Figure 1. The OMT geometry, including port definitions, waveguide dimensions, and additional design parameters.

applications. We also discuss a gold-plating technique to reduce the impact of the troublesome *H*-plane gaps that often occur in machined waveguide pieces. Compared with the design presented in [20], our OMT provides comparable performance, while requiring optimization of fewer geometric parameters and fabrication with fewer machining steps, and demonstrates a much better agreement between simulation and measurement results.

2. OMT Design

The OMT design features three waveguide ports. The vertical (V) and horizontal (H) ports are standard rectangular waveguides, while the common port is a square waveguide, supporting both V- and H-polarized modes. The V and H branches are transitioned from rectangular to square, and the three square waveguide sections intersect at a T junction. To discuss the characteristics of the OMT by referring to its scattering parameters, the V port is defined as port 1, the H port as port 2, the V-polarized common port mode as port 3, and the H-polarized common port mode as port 4. In this manner, the OMT may be treated as a four-port network [21]. The geometry of the design is shown along with these port definitions and the relevant dimensions in Figure 1. The main innovation in this design is the single-step discontinuity in port 1 that creates a resonant section to effectively transfer the power from port 1 to port 3, while presenting a short circuit seen by the field in port 2.

The band of interest for this design is 220 GHz to 230 GHz. The WR-03 waveguide size was chosen to ensure that the cut-off frequency of the TM_{11} and TE_{11} square waveguide modes (245 GHz) is above the operation band.

3. Simulation

The OMT was designed with the assistance of electromagnetic simulations in Ansys HFSS, version 19.5, using the finite element method. The waveguide walls were modeled as finite conductivity boundaries to reflect the expected losses. In addition to the fundamental TE_{10} mode, the first higher order mode was also included at each of the wave ports to observe and minimize any possible coupling to those modes.

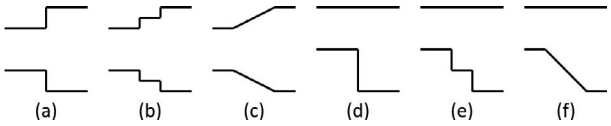

Figure 2. Different types of simple transitions from rectangular to square waveguides (shown in *E* plane). (a) Single step, (b) double step, (c) tapered, (d) asymmetric single step, (e) asymmetric double step, and (f) asymmetric tapered.

Different types of transitions from square to rectangular waveguide were considered for both the V and H ports. Step transitions can be designed using modal analysis, but such analytical methods do not provide the needed accuracy [22]. Several such transitions are depicted in Figure 2. Each transition was first optimized to maximize transmission and minimize reflection. Then various combinations of transitions were integrated into the OMT, and the positions along the waveguides were optimized to maximize transmission between ports 1 and 3, and ports 2 and 4, as well as to minimize reflection at all four ports. The configuration shown in Figure 1 provided the most favorable performance characteristics out of the transition combinations tested. It features symmetric tapered and single-step transitions at the H and V ports, respectively.

A tapered transition is expected to provide better performance over a wider band than a transition with discrete steps. In theory, the reflection should be minimized for taper lengths (d_3) of integer multiples of half-guide wavelengths [23]. The length chosen here is approximately a full guide wavelength at the center frequency of our band. For fabrication with a mill axis along the vertical direction, a tapered transition is not possible for the V port; thus, a stepped transition must be used instead. This limits the bandwidth of the OMT for V-polarized signals. The single-step transition was found to provide comparable performance to the double step (in the context of the full OMT) and was therefore chosen for its simplicity. The lengths d_1 and d_2 can be thought of as free parameters to assist in impedance matching. The V and H ports see the impedances of two sections of waveguide in parallel; d_1 can be used to help match the H port, while d_2 can be used to help match the V port.

The dimensions of the final optimized OMT design are $a = 0.8636$ mm, $b = 0.4318$ mm, $d_1 = 0.8636$ mm, $d_2 = 0.1270$ mm, and $d_3 = 1.8288$ mm. The lengths of the three waveguide sections referenced to the center of the T junction are 9.525 mm for the V port and 13.970 mm for H and common ports (for the purpose of fabrication).

4. Fabrication

The OMT was fabricated using CNC milling to carve the waveguides into blocks of brass. The milling machine is a Bridgeport model M-105k retrofitted with the ProtoTRAK M3 control system. Typical accuracy

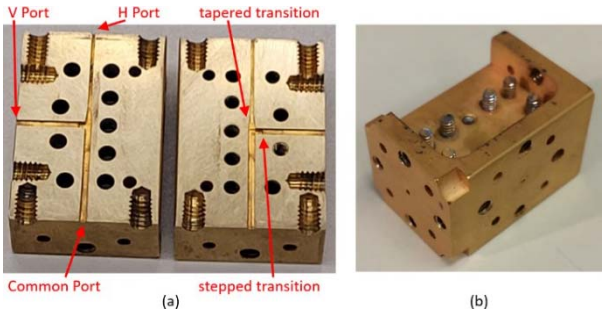

Figure 3. Photographs of (a) the adjoining surfaces of the two brass blocks with the tiny milled waveguide features highlighted and (b) the finished OMT after assembly and gold plating.

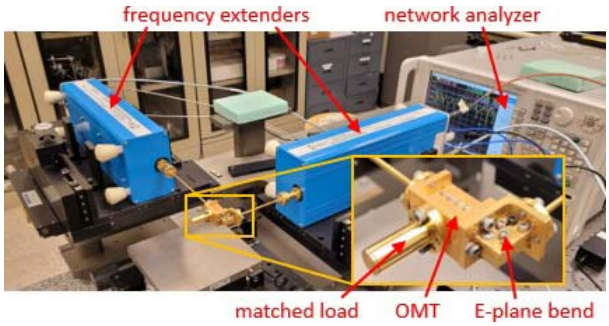

Figure 4. Photographs of the OMT *S*-parameter measurement setup.

along a straight line is 0.002 in (50 μm) over 5 in (127 mm) travel.

A symmetric split-block assembly was used, with a split plane through the middle of all three ports. On each block, two milling steps were used: the first with a depth of $a/2$ to form the common and H-port waveguides and V-port matching section, and the second with a depth of $b/2$ to complete the V-port waveguide. Screw holes were drilled and tapped to attach the two blocks to each other. Guide pins were used to assist in alignment of the blocks. Finally, once the OMT was assembled to satisfaction, flanges were added around the three ports to mate the OMT to other waveguide components.

When an OMT is assembled, any small gap between the surfaces allows energy to leak out of the waveguide. To minimize the insertion loss, the adjoining faces of each block were polished using a manual lapping table prior to milling the waveguides, providing a smooth and flat surface to make a connection without any gaps. Additionally, the assembled OMT was plated with an electroless gold-plating solution to fill any gaps caused by small scale roughness. These steps were found to significantly reduce the insertion loss to close to 1 dB. Even commercial injection molded through waveguide components at the WR-03 size and a similar length will typically exhibit insertion loss of this order. Figure 3 displays some photographs of the OMT.

5. Measurement

The measurement setup for characterization of the OMT performance includes an Agilent N5245 4-port PNA-X performance network analyzer configured with two frequency extension modules. This system has WR-03 waveguide interfaces and allows for measurement of the scattering matrices of two-port networks at frequencies up to 325 GHz. The OMT scattering parameters were measured in sets of two ports at a time. To facilitate connections to the necessary port combinations, the extenders were positioned with 90° of rotation between them, and a 90° *E*-plane waveguide bend was included within the calibration. The measurement setup is shown in Figure 4.

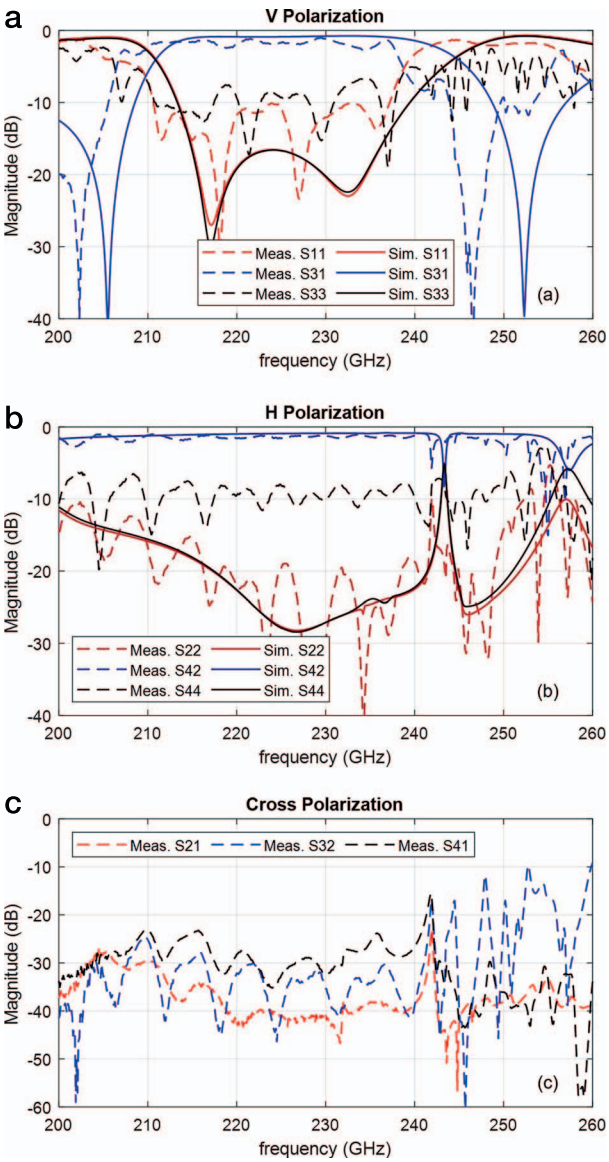

Figure 5. The *S*-parameters of the OMT, with measurements compared to simulation results. For clarity, the *S*-parameters are split up into those related to (a) V polarization, (b) H polarization, and (c) cross polarization (simulation is below –60 dB and therefore not shown).

Table 1. Comparison of performance and fabrication complexity to other OMTs

References	This work	[6]	[7]	[20][a]	[9]	[13]	[15, 16]	[17]
Junction type	T	T	T	T	Reverse coupling	Bøifot	Turnstile	Turnstile
Center frequency (GHz)	224	90	550	215	440	440	235	225
Bandwidth (%)	11.8	27	18	4.7	26	26	30	49
Insertion loss (dB)	<2.7	<2	<8	<4	<2.7	<1.8	<0.8	<0.8
Return loss (dB)	>10	>24	>17	>9	>10	>20	>12	>16
Isolation (dB)	>30	>37	>19 to 28[b]	>30	>25	>29	>25	>20
Metallic blocks	2	2	2	2	2	2	4	3[c]
Machined waveguide sections per block[d]	5	15	11	7	>20	>20	>40	3[c]
Fabrication complexity[e]	Low	Medium	Medium	Medium	High	High	High	High

[a] Values based on plot of measured scattering coefficients presented over the cited 210 GHz to 220 GHz band; the authors claim different values.
[b] Three prototypes were measured with differing isolation due to block misalignment.
[c] A silicon microfabrication process was used; in this case, read as three substrate layers and three etched waveguide sections per substrate layer.
[d] Number of waveguide sections of different dimensions requiring additional programming or retooling or both.
[e] Medium complexity refers to cases that have waveguide sections with irregular geometries; high complexity refers to designs that have curved waveguide sections, out of plane milling, or the need to flip and align the metal block to complete milling the piece.

Figure 5 shows several plots comparing the measured and simulated scattering parameters of the OMT (simulated cross polarization is not shown because it is below –60 dB). When either the V or H port was not used for a particular *S*-parameter measurement, it was terminated with a waveguide fixed matched load. A horn antenna was used to approximate an impedance match at the common port when measuring isolation between the V and H ports, because no square waveguide matched load was available.

The return loss is better than 10 dB at the V and H ports over the band from 210.7 GHz to 237.1 GHz, which represents a bandwidth of 11.8%. The band of operation was observed to have slightly shifted downward compared with the simulation due to machining tolerance. Over the 210.7 GHz to 237.1 GHz band, the average V-polarized insertion loss is 1.7 dB, while the average H-polarized insertion loss is 1.4 dB. The maximum insertion loss for either polarization is 2.7 dB. The V- to H-port isolation is at least 30 dB. Cross-polarization discrimination (i.e., how much V-polarized signal at the V port appears due to an H-polarized excitation at the common port) is greater than 23 dB. Note that it is impossible to measure S_{43} and S_{34}, as the two ports are coincident in space, but these parameters hold no practical significance.

Based on the measured common port return loss, there is a significant contribution to the OMT's measured insertion loss purely due to reflection at the mismatched (square-to-rectangular) common port. Back-to-back transmission measurements were made in which this OMT and a second similar one were connected at their common ports. The average back-to-back insertion loss was 2.3 dB for V polarization and 1.6 dB for H polarization. Assuming equal contribution from each OMT, this gives an estimated insertion loss of 1.15 dB and 0.8 dB for V and H polarizations, approaching the reasonable limit.

The measured performance of this OMT is compared with other OMT designs at similar millimeter-wave and terahertz frequency bands in Table 1. With the exception of bandwidth, this design's performance characteristics are comparable to the others', while requiring fewer machined waveguide sections per block and avoiding irregular geometries and bends.

6. Conclusion

An OMT with a simple structure was designed and fabricated for operation at high millimeter-wave frequencies (in particular, the 220 GHz to 230 GHz band). The measured performance indicates a bandwidth of about 12%, with better than 10 dB return loss, 23 dB polarization discrimination, and 30 dB isolation. Through lapping of the adjoining split-block surfaces and electroless gold plating, the insertion loss has been minimized to less than 1.7 dB, on average, and possibly closer to 1 dB, based on back-to-back transmission measurements. This OMT design minimizes structural complexity so that it can be fabricated using CNC machining without requiring top-of-the-line equipment. We were able to build the OMT at an estimated unit machining cost of $2400, significantly less than the price tag of commercial OMTs at this band (∼$15,000). Fabricated OMTs were used in the front ends of two *J*-band polarimetric radar systems for backscattering phenomenology in support of the automotive industry.

7. References

1. K. Sarabandi and E. S. Li, "Characterization of Optimum Polarization for Multiple Target Discrimination Using Genetic Algorithms," *IEEE Transactions on Antennas and Propagation*, **45**, 12, December 1997, pp. 1810-1817.
2. K. Sarabandi and E. S. Li, "Polarimetric Characterization of Debris and Faults in the Highway Environment at Millimeter-Wave Frequencies," *IEEE Transactions on Antennas and Propagation,* **48**, 11, November 2000, pp. 1756-1768.
3. A. A. Alaqeel, A. A. Ibrahim, A. Y. Nashashibi, H. N. Shaman, and K. Sarabandi, "Experimental Characterization of Multi-Polarization Radar Backscatter Response of Vehicles at J-Band," *IEEE Transactions on Intelligent Transportation Systems*, **20**, 9, November 2018, pp. 3337-3350.
4. Y. Kawano, H. Matsumura, S. Shiba, M. Sato, T. Suzuki, et al., "230-240 GHz, 30 dB Gain Amplifier in INP-

HEMT for Multi-10 Gb/s Data Communication Systems," 2013 IEEE Compound Semiconductor Integrated Circuit Symposium, Monterey, CA, USA, October 13–16, 2013, pp. 1-4.
5. K. Sarabandi, A. Jam, M. Vahidpour, and J. East, "A Novel Frequency Beam-Steering Antenna Array for Submillimeter-Wave Applications" *IEEE Transactions on Terahertz Science and Technology*, **8**, 6, August 2018, pp. 654-665.
6. A. Dunning, S. Srikanth, and A. R. Kerr, "A Simple Orthomode Transducer for Centimeter to Submillimeter Wavelengths," 20th International Symposium on Space Terahertz Technology, Charlottesville, VA, USA, April 20–22, 2009, pp. 191-194.
7. T. J. Reck and G. Chattopadhyay, "A 600 GHz Asymmetrical Orthogonal Mode Transducer," *IEEE Microwave and Wireless Component Letters*, **23**, 11, November 2013, pp. 569-571.
8. O. A. Peverini, R. Tascone, G. Virone, A. Olivieri, and R. Orta, "Orthomode Transducer for Millimeter-Wave Correlation Receivers," *IEEE Transactions on Microwave Theory and Techniques,* **54**, 5, May 2006, pp. 2042-2049.
9. C. Groppi, A. Navarrini, and G. Chattopadhyay, "A Waveguide Orthomode Transducer for 385-500 GHz", Millimeter, Submillimeter, and Far-Infrared Detectors and Instrumentation for Astronomy V, San Diego, CA, USA, July 15, 2010, pp. 1-11.
10. G. Chattopadhyay and J. E. Carlstrom, "Finline Ortho-Mode Transducer for Millimeter Waves," *IEEE Microwave and Guided Wave Letters*, **9**, 9, September 1999, pp. 339-341.
11. A. M. Bøifot, E. Lier, and T. Schaug-Pettersen, "Simple and Broadband Orthomode Transducer," *IEE Proceedings H (Microwaves, Antennas, and Propagation)*, **137**, 6, December 1990, pp. 396-400.
12. G. Narayanan and N. Erickson, "Full-Waveguide Band Orthomode Transducer for the 3 mm and 1 mm Bands," 14th International Symposium on Space Terahertz Technology, Tucson, AZ, USA, April 22–24, 2003, pp. 508-512.
13. M. Kamikura, M. Naruse, S. Asayama, N. Satou, W. Shan, et al., "Development of a Submillimeter Double-Ridged Waveguide Ortho-Mode Transducer (OMT) for the 385–500 GHz Band," *Journal of Infrared, Millimeter, and Terahertz Waves*, **31**, June 2010, pp. 697-707.
14. A. Navarrini and R. L. Plambeck, "A Turnstile Junction Waveguide Orthomode Transducer," *IEEE Transactions on Microwave Theory and Techniques*, **54**, 1, January 2006, pp. 272-277.
15. A. Navarrini, R. L. Plambeck, and D. Chow, "A Turnstile Junction Waveguide Orthomode Transducer for the 1 mm Band," 16th International Symposium on Space Terahertz Technology, Gothenburg, Sweden, May 2–4, 2005, pp. 519-523.
16. A. Navarrini, A. Bolatto, and R. L. Plambeck, "Test of 1 mm Band Turnstile Junction Waveguide Orthomode Transducer," 17th International Symposium on Space Terahertz Technology, Paris, France, May 10–12, 2006, pp. 99-102.
17. A. Gomez-Torrent, U. Shah, and J. Oberhammer, "Compact Silicon-Micromachined Wideband 220–330-GHz Turnstile Orthomode Transducer," *IEEE Transactions on Terahertz Science and Technology*, **9**, 1, January 2019, pp. 38-46.
18. G. Valente, A. Navarrini, F. Schaefer, P. Serres, and F. Thome, "Architecture of Highly Integrated Cryogenic Active Planar Orthomode Transducer for the 3-mm Band," 2018 2nd URSI Atlantic Radio Science Meeting, Gran Canaria, Spain, May 28–June, 1, 2018, pp. 1-4.
19. T. J. Douglas, A. Y. Nashashibi, and K. Sarabandi, "A 230 GHz Orthomode Transducer with Simple Fabrication Steps," IEEE International Symposium on Antennas and Propagation, Singapore, Singapore, December 2021, pp. 463-464.
20. T. Qin, X. Q. Lin, and Y. X. Kang, "A Simple Terahertz Orthomode Transducer Based on Equivalent Circuits Analysis," 2020 IEEE MTT-S International Microwave Workshop Series on Advanced Materials and Processes for RF and THz Applications, Suzhou, China, July 29–31, 2020, pp. 1-3.
21. K. Sarabandi and F. T. Ulaby, "A Convenient Technique for Polarimetric Calibration of Single-Antenna Radar Systems," *IEEE Transactions on Geoscience and Remote Sensing*, **28**, 6, November 1990, pp. 1022-1033.
22. K. Sarabandi, *Foundations of Applied Electromagnetics*, Ann Arbor, MI, University of Michigan Press, 2022.
23. G. L. Ragan, "Transition Units," in G. L. Ragan (ed.), *Microwave Transmission Circuits*, 1st Ed., New York, McGraw-Hill, 1948, Chapter 6.